

Modelling thermal recycling occurring in groundwater heat pumps (GWHPs)

Original

Modelling thermal recycling occurring in groundwater heat pumps (GWHPs) / Casasso, Alessandro; Sethi, Rajandrea. -
In: RENEWABLE ENERGY. - ISSN 0960-1481. - ELETTRONICO. - 77:(2015), pp. 86-93.
[10.1016/j.renene.2014.12.003]

Availability:

This version is available at: 11583/2583144 since:

Publisher:

Elsevier

Published

DOI:10.1016/j.renene.2014.12.003

Terms of use:

This article is made available under terms and conditions as specified in the corresponding bibliographic description in the repository

Publisher copyright

(Article begins on next page)

Modelling thermal recycling occurring in Groundwater Heat Pumps (GWHPs)

Authors: Alessandro Casasso, Rajandrea Sethi *

* corresponding author

DIATI – Politecnico di Torino, corso Duca degli Abruzzi 24, 10129 Torino (Italy)

Telephone number: +39 0110907735

alessandro.casasso@polito.it , rajandrea.sethi@polito.it

Highlights

- Thermal recycling should be studied when dimensioning GWHPs.
- The potential flow theory accurately reproduces the hydraulics of a GWHP.
- The potential flow theory applied to GWHPs was implemented in a MATLAB™ function.
- A practical formula was deduced for the calculation of thermal recycling in a GWHP.
- TRS and the practical formula were validated through simulations with FEFLOW™.

Abstract

10

11 The performance of a Ground Water Heat Pump (GWHP) is often impaired by the thermal
12 recycling between the injection and the extraction well(s), and hence this phenomenon
13 should be evaluated in the design of open loop geothermal plants. The numerical flow and
14 heat transport simulation of a GWHP requires an expensive characterization of the aquifer
15 to obtain reliable input data, which is usually not affordable for small installations. To
16 provide a simple, fast and inexpensive tool for preliminary and sensitivity analyses, an
17 open-source numerical code was developed, which solves the hydraulic and thermal
18 transport problem of a well doublet in the presence of a subsurface flow. The code, called
19 TRS (Thermal Recycling Simulator), is based on a finite-difference approximation of the
20 potential flow theory. The method was validated through the comparison with flow and
21 heat transport simulations with FEFLOW. Subsequently, TRS was run with different values
22 of the aquifer and plant parameters. The correlation observed between some characteristic
23 non-dimensional quantities permitted an empirical correlation to be developed, that
24 describes the time evolution of the extracted water temperature. An example is given for
25 the use of the numerical code and the formula in the dimensioning of an open loop
26 geothermal plant.

27

Keywords

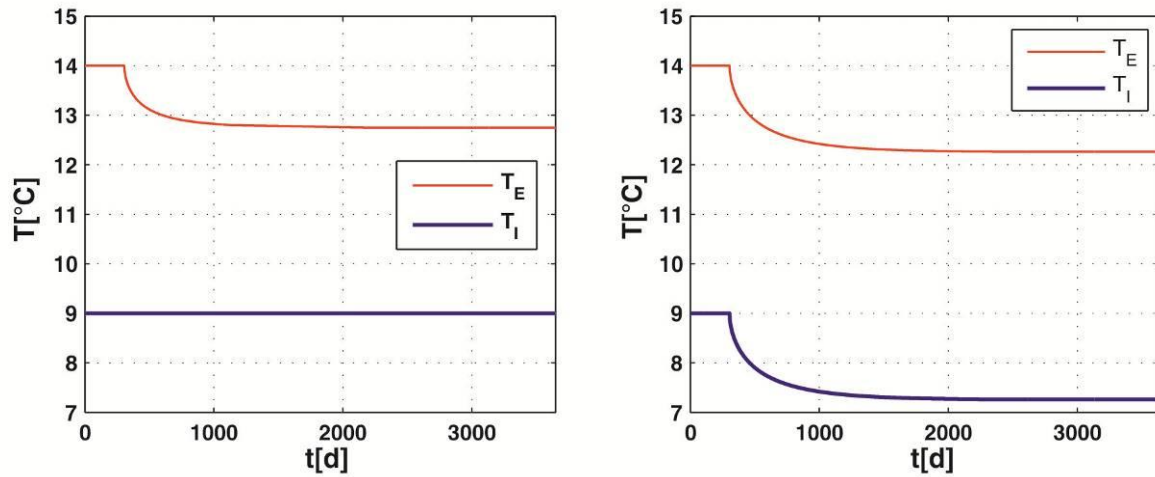
28 Ground Water Heat Pump; groundwater; geothermal; thermal recycling; thermal
29 breakthrough; potential flow theory.

30

31 **1. Introduction**

32 Geothermal Heat Pump (GHP) installations are spreading fast all over the world, with a
33 total installed power of 33 GW [1]. Half of the world's shallow geothermal energy
34 production takes place in Europe, with a positive occupational and environmental impact,
35 as 7000 people are employed in this sector [2] and a reduction of 5.5 Mton CO₂ per year is
36 achieved by using GHPs instead of more carbon-intensive technical solutions [3]. GHPs
37 are divided into closed loop or Ground Coupled Heat Pumps (GCHPs), where a heat
38 carrier fluid circulates in a pipe circuit buried in the ground, and open loop or Groundwater
39 Heat Pumps (GWHPs), where the thermal exchange takes place directly on the extracted
40 groundwater, which is then usually re-injected into the same aquifer [4]. While closed loop
41 systems (i.e. Borehole Heat Exchangers, energy piles, earth coils) are based mainly on
42 conductive heat exchange with the surrounding ground and, to a lesser extent, advection
43 and dispersion [5-7], the thermal exchange for GWHPs is mostly advective [8]. Since water
44 is usually reinjected after the heat exchange with the evaporator/condenser, a plume of
45 chilled/warmed groundwater around the injection well is generated, which can return to the
46 abstraction well with a gradual worsening of the performance of the system. This
47 phenomenon was firstly observed in the Thirties in Long Island (New York), as re-injection
48 was prescribed to avoid the depletion of the shallow coastal aquifer [9], and it was then
49 either called thermal breakthrough, short-circuit, feedback, recycling etc., usually without
50 any clear distinction. Recently, however, Milnes and Perrochet [10] defined thermal
51 feedback as occurring when the value of the injection temperature is imposed, and thermal
52 recycling when a temperature difference between abstraction and injection is set (Fig.1).

53



54

55 **Fig. 1 – Difference between thermal feedback (on the left) and thermal recycling (on the right).**

56

57 According to this classification, thermal feedback has been studied for a long time, since
 58 Gringarten and Sauty [11] developed a formula for the calculation of the temperature
 59 variation in the abstraction well through time. Instead, thermal recycling has only been
 60 studied more recently, since its formulation is more complicated from the mathematical
 61 point of view. However, the time it takes for reinjected water to reach the extraction well,
 62 which is hereby called thermal breakthrough time (t_{tb}), does not vary depending on the
 63 injection temperature. Lippmann and Tsang [12] calculated its value for three different
 64 hydrogeological setups: no groundwater flow, regional flow from the injection to the
 65 abstraction well and regional flow from the abstraction to the injection well.

66 While thermal breakthrough inevitably occurs in the first two cases, in the third case it is
 67 not observed if:

68
$$X = \frac{2Q_w}{\pi b k J L} < 1$$

69

Equation 1

70 where Q is the flow rate exchanged by the wells [$m^3 s^{-1}$], b is the aquifer thickness [m], k
 71 is the hydraulic conductivity of the aquifer [ms^{-1}], J is the hydraulic gradient [-] and L is the
 72 distance between the wells [m].

73 This equation is only valid for groundwater flow aligned with the well doublet, and the
74 parameter x is the measure of how strong will the thermal breakthrough be. The minimum
75 value of L required to cope with the criterion of Eq.1 is too large for most GWHP well
76 doublets, but the breakthrough time t_{tb} could be longer than the duration of a heating or
77 cooling season, thus avoiding the occurrence of this phenomenon. In addition, the thermal
78 recycling can develop over long time scales and/or at a low rate, permitting the plant
79 operation to be continued with a slight reduction of COP (Coefficient Of Performance) or of
80 the EER (Energy Efficiency Ratio). For these reasons, the main focus of the design of an
81 open loop geothermal heat pump is not determining whether the thermal breakthrough is
82 theoretically possible or not, but whether the impact of thermal recycling is sustainable
83 during the heating/cooling seasons and through years. For this task, transient numerical
84 modelling would be the optimal solution, both with programs able at modelling coupled
85 flow and heat transport, like FEFLOW™ [13-16], or flow and solute transport, like
86 MODFLOW, applying the similarity between solute and heat transport [17-19]. In fact,
87 these programs can simulate complicated hydrogeological setups and well arrangements,
88 variable thermal loads, variable flow rates, and optimize the arrangement of the wells and
89 the flow rate patterns. On the other hand, a thorough characterization of the aquifer, which
90 would be necessary for an appropriate use of these softwares, is not affordable for small
91 GWHPs and hence it is usually not performed. In these cases, it is advisable to use
92 simplified models analyzing a broad range of conditions, rather than using sophisticated
93 models with arbitrarily imposed input data. Poppei et al. [20] developed a software called
94 GED (Groundwater Energy Design) which calculates the spatial distribution of
95 groundwater temperatures around a GWHP with simplified models, but not the time
96 evolution of the extracted and injected water temperatures. The analytical formulae
97 reported in Stauffer et al. [21] can be used to calculate the thermal alteration in the

98 extraction well if the injection temperature is known *a priori* (thermal feedback). No
99 simplified methods were found in the literature to simulate the thermal recycling.
100 A numerical code was therefore developed, starting from the modelling framework of the
101 potential flow theory described by Strack [22] and Luo and Kitanidis [23] that can be
102 adopted for the calculation of velocities and pathlines of a geothermal well doublet. The
103 use of particle tracking (PT) for the design of a GWHP was also proposed by Ferguson
104 [24], who calculated the thermal feedback with a finite-difference flow and solute transport
105 numerical models (MODFLOW with MODPATH) to simulate the thermal feedback with well
106 schemes more complex than a doublet. These articles above provided the conceptual
107 basis for the thermal recycling modelling carried out in this study, where the potential flow
108 theory was used to implement the TRS (Thermal Recycling Simulator) MATLAB™
109 function, able to determine the time series of the extracted water temperature in a GWHP.
110 The adopted numerical method was validated through finite-element simulations
111 developed under FEFLOW™, achieving a good agreement between computed water
112 temperatures, in a wide range of parameter values (well distance, flow rate, hydraulic
113 conductivity etc.) that can be met in real installations. Subsequently, TRS has been used
114 for a larger number of simulations, in order to understand how the thermal recycling
115 evolves depending on these quantities. The time series of the abstraction well temperature
116 have been analyzed, deriving an empirical correlation that can be used to assess the
117 feasibility of a GWHP setup. Finally, an example of the use of the formula and of TRS is
118 given in this paper, comparing their results with those obtained with FEFLOW™.

119 **2. Derivation of the numerical code**

120 The thermal recycling in a GWHP is caused by the hydraulic recirculation from the
121 injection to the extraction well(s), and hence it is necessary to study the path and the travel
122 times of water injected into the aquifer, discretizing it into fractions and assessing which

123 ones will flow downstream and which ones will be captured by the pumping well(s) located
 124 upstream. The potential flow theory of Strack [22] can be effectively applied for this
 125 purpose, provided that some simplifying assumptions are made (homogeneous aquifer
 126 properties distributions, constant flow rate etc.). In this way, the superposition principle can
 127 be applied in the modelling of two wells, one with a positive (extracted) flow rate Q_w and
 128 one with a negative (injected) flow rate $-RF \cdot Q_w$ (with $RF \leq 1$ being the fraction of the
 129 extracted flow rate which is reinjected), and a homogeneous groundwater flow \bar{Q}_{gw} with a
 130 generic orientation ϑ . Partial reinjection is quite uncommon, and therefore the analyses
 131 conducted in this study are focused on the case of a full reinjection ($RF = 1$), which is the
 132 usual solution adopted in these plants. Nevertheless, the program is also capable of
 133 dealing with partial reinjection, which will be considered in the mathematical derivation
 134 presented in this chapter.

135 The complex potential of a well doublet in the presence of a regional flow can be
 136 formalized as follows [23]:

$$137 \quad \Omega(z) = \frac{Q_w}{2\pi} \log(z - z_E) - \frac{RF \cdot Q_w}{2\pi} \log(z - z_I) - \bar{Q}_{gw} z$$

138 **Equation 2**

$$139 \quad Q_{gw} = k J b e^{i\vartheta}$$

140 **Equation 3**

141 where Q_w is the extraction well flow rate [$m^3 s^{-1}$], z_E and z_I are the planar positions of the
 142 extraction and the injection wells [m] expressed as complex numbers ($z = x + iy$), \bar{Q}_{gw} is the
 143 complex conjugate of the groundwater flow vector [$m^2 s^{-1}$], k is the hydraulic conductivity of
 144 the aquifer [ms^{-1}], J is the modulus of the hydraulic gradient in the aquifer [-], b is the
 145 thickness of the aquifer [m] and ϑ is the direction angle of the groundwater flow

146 (measured counter-clockwise with respect to the conjunction between the extraction and
147 the injection well).

148 The vector of the effective velocity field is a function of the spatial derivate of the complex
149 potential, which in turns depends on the planar position z :

$$150 \quad v_e(z) = -\frac{1}{b \cdot n_e} \frac{d\Omega}{dz} = \frac{1}{b \cdot n_e} \cdot \left[\frac{Q_w}{2\pi} \left(\frac{RF}{z - z_i} - \frac{1}{z - z_E} \right) + \bar{Q}_{gw} \right]$$

151 **Equation 4**

152 The spatial distribution of groundwater effective velocities permits particles to be tracked
153 backward or forward from a generic starting point, by means of finite difference schemes.

154 Since the saturated aquifer thickness b is considered as homogeneous and constant,
155 Eq.4 is valid, strictly speaking, only for confined aquifers: nevertheless, the influence of the
156 variation of the saturated thickness on groundwater velocities in unconfined aquifers is not
157 appraisable when computing particle travel times.

158 A forward particle tracking procedure was implemented in a MATLAB™ numerical code
159 called TRS (Thermal Recycling Simulator), in order to draw the pathlines and calculate the
160 travel times of particles starting from the injection well. Considering a uniform radial
161 distribution of the flow rate, the injection well pipe wall can be subdivided into N sectors
162 with equally spaced particles, each one separated by an angle of $2\pi/N$ radians and
163 representative of $1/N$ of the total flow rate circulated. Through the calculation of the
164 pathlines, it is possible to ascertain how many of them will reach the extraction well and,
165 by sorting the particle travel times, the time series of the recycled flow rate fraction
166 $RR(t)$ can be derived.

167 The PT procedure explained so far only takes into account the hydraulic particle travel
168 times, neglecting the fact that the heat exchange between the injected water and the
169 aquifer results in a slower propagation of the thermal alteration with respect to
170 groundwater. Since the transport equations of solute and heat have a similar form, the

171 thermal retardation factor [25] can be defined, which is the ratio between hydraulic and
 172 thermal particle effective velocities:

$$173 \quad R_{th} = 1 + \frac{(1-n_e)\rho_s c_s}{n_e \rho_w c_w} \geq 1$$

174 **Equation 5**

$$175 \quad v_{e-th}(z) = \frac{v_e(z)}{R_{th}}$$

176 **Equation 6**

177 Depending on the velocity flow field described by Eq.4 and 6, a maximum number of
 178 particles $n_{max} \leq N$ can return to the extraction well, each one after a time $t_p(i)$ which is
 179 computed by TRS.

180 The maximum flow rate fraction which is recycled between the wells is:

$$181 \quad RR_{max} = \frac{n_{max}}{N}$$

182 **Equation 7**

183 At the time $t \geq t_p(n)$, n particles have reached the extraction well, and the water
 184 temperature is therefore:

$$185 \quad T_E(t) = (1 - RR_{max}) \cdot T_0 + \left(RR_{max} - \frac{n}{N} \right) \cdot T_0 + \sum_{i=1}^n \frac{1}{N} T_i(t - t_p(i))$$

186 **Equation 8**

187 The three terms of Eq. 8 respectively represent the following flow rate fractions:

- 188 - a constant fraction which is always extracted from upstream, and therefore it is not
- 189 thermally altered;
- 190 - the variable thermally unaltered flow rate fraction, which diminishes through time
- 191 reaching a value of zero as the asymptote RR_{max} is reached and n_{max} particles on a
- 192 total of N have returned to the abstraction well;

193 - the flow rate fraction which comes from the injection well, which is composed of
 194 $n(t)$ particles, each one started at a time $t-t_p(i)$ with a different injection
 195 temperature:

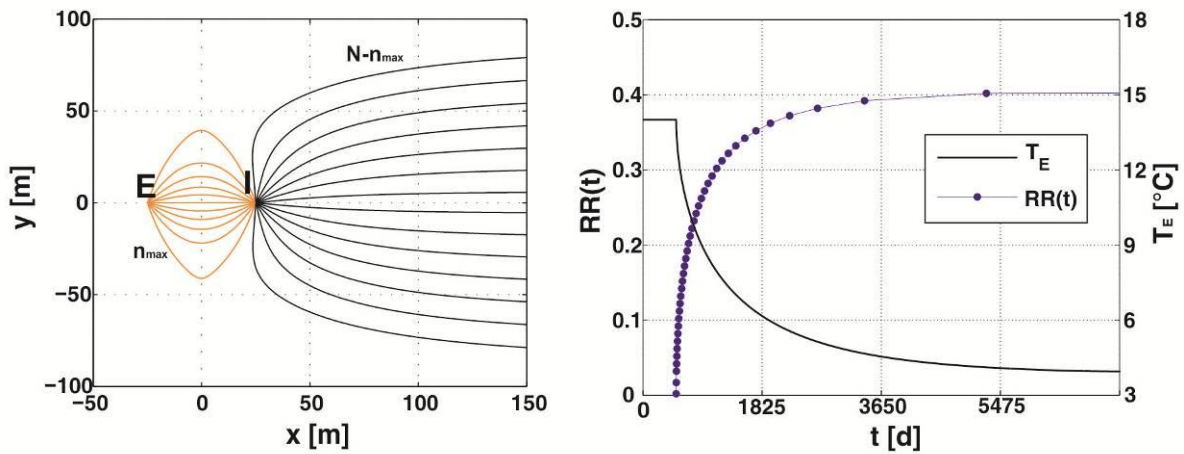
$$196 \quad T_i(t-t_p(i)) = T_E(t-t_p(i)) + \Delta T$$

197 Equation 9

198 where ΔT is the constant temperature difference between the injection and the
 199 extraction wells.

200 The TRS code is available at the website of Groundwater Engineering research group of
 201 Politecnico di Torino [26], and further details about the implementation of this
 202 mathematical model in TRS are reported in the supporting information, while the
 203 conceptual steps of the procedure described in this chapter are summarized in Fig. 2.

204



205

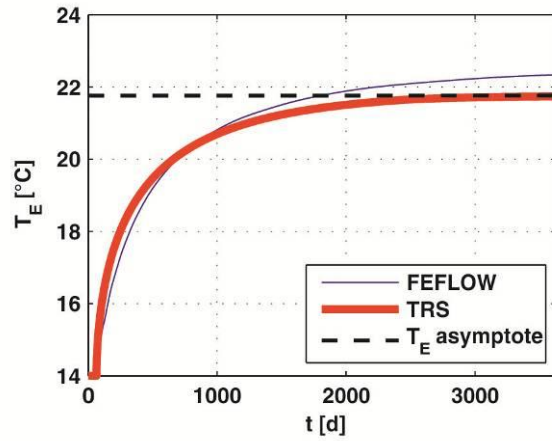
206 **Fig. 2 – Graphical synthesis of the procedure implemented in TRS. On the left, the particle tracking is**
 207 **shown, with n_{\max} particles being recycled between the wells and $N-n_{\max}$ particles flowing**
 208 **downstream from the injection well. On the right, the recycled fraction $RR(t)$ is plotted with the**
 209 **ordinate on the left (dotted blue line), while the extracted water temperature is plotted with the**
 210 **ordinate on the right (black line).**

211

212 3. Validation of the Thermal Recycling Simulator

213 The method previously described was validated through simulations with the 3D numerical
214 flow and heat transport modelling program FEFLOW™ [14]. This software includes a
215 special package (OpenLoop IFM plugin [27]) for simulating a well doublet with a prescribed
216 (constant or variable) temperature difference. The parameter values and the numerical
217 settings adopted in the simulations for the verify of TRS are summarized on Tab. 1. A very
218 large rectangular mesh (5x3 km) was built around the well doublet to avoid boundary
219 effects. The aquifer was set as unconfined, and the hydraulic gradient was imposed with
220 appropriate boundary conditions at each slice. A very low thermal conductivity
221 ($\lambda_s = 0.01 \text{ Wm}^{-1} \text{ K}^{-1}$) was assigned to the solid matrix of the aquifer, with the aim of
222 reproducing the simplifying assumption of purely advective heat transport. An assessment
223 of the error introduced by neglecting the heat conduction and dispersion is included in the
224 supporting information, proving that this leads to an overestimation of the thermal
225 alteration of the extracted water. A total number of 13 simulations was run, with different
226 aquifer parameters, well distances and flow rates, in order to cover a wide range of case
227 studies. The non-dimensional parameter X , which represents the strength of the thermal
228 recycling, varies between 1.27 (very weak) and 63.66 (very strong). A graphical
229 comparison of the results of FEFLOW™ and TRS is reported in Fig. 3, while further
230 analyses of the agreement between the results of these tools are reported in the
231 supporting information. The thermal recycling is reproduced accurately by TRS for small
232 and medium values of X (i.e. less than 10), which are the most likely in GWHP plants,
233 while a worse agreement is obtained for large values (larger than 10), which are however
234 not met in reality.

235



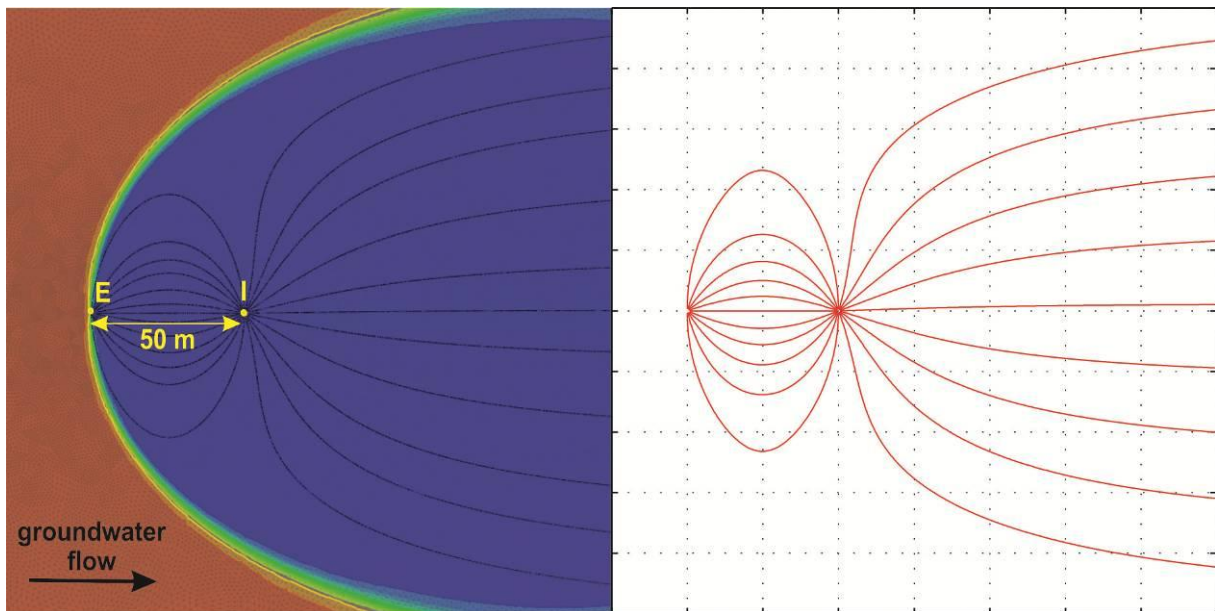
236

237 **Fig. 3 – Example of a graphical comparison of extracted water temperatures calculated by the**
 238 **FEFLOW™ model and by TRS. Further similar plots are reported in the supporting information.**

239

240 The streamlines calculated with TRS according to the potential flow field were compared
 241 with the ones calculated by FEFLOW™, and a good agreement is observed between them
 242 (Fig. 4).

243



244

245 **Fig. 4 – Comparison between particle tracking in the FEFLOW™ model (on the left) and with the**
 246 **finite-difference potential flow theory implemented in TRS (on the right).**

247

248 Two other quantities can be examined to check the correctness of the mathematical
 249 model: the thermal breakthrough time t_{tb} , which is the shortest particle travel time, and the
 250 maximum recirculated flow rate fraction RR_{\max} . Both these quantities are described by
 251 explicit analytical formulae reported in Milnes and Perrochet [10]:

$$252 \quad t_{tb} = R_{th} \cdot \frac{n_e L}{kJ} \cdot \left(\frac{X}{\sqrt{X-1}} \tan^{-1} \left(\frac{1}{\sqrt{X-1}} \right) - 1 \right)$$

253 **Equation 10**

$$254 \quad RR_{\max} = \frac{2}{\pi} \left(\tan^{-1}(\sqrt{X-1}) - \frac{\sqrt{X-1}}{X} \right)$$

255 **Equation 11**

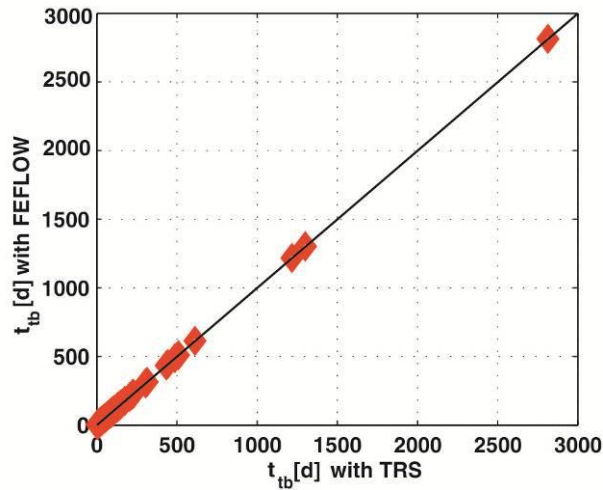
256

257 The scatterplots of the values of t_{tb} and RR_{\max} calculated analytically and numerically for a
 258 large set of simulations are reported in Fig. 5 and Fig. 6 respectively, showing a good
 259 alignment. TRS also correctly simulates the asymptotical maximum thermal alteration
 260 reached in the case of thermal recycling, which is also described by an analytical formula
 261 [9]:

$$262 \quad T_E(\infty) - T_0 = \frac{RR_{\max}}{1 - RR_{\max}} \Delta T$$

263 **Equation 12**

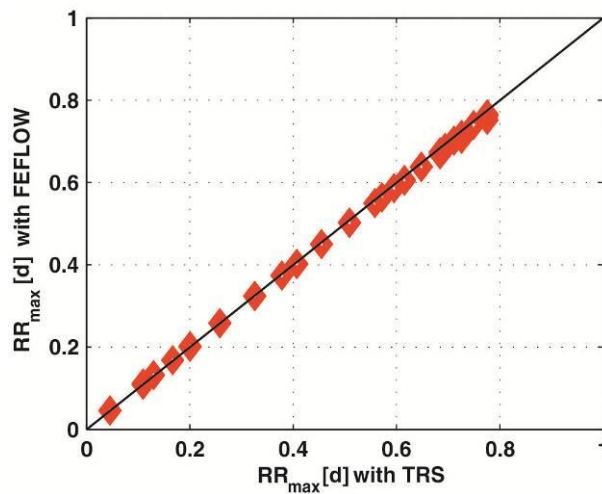
264



265

266 Fig. 5 – Scatterplot of thermal breakthrough times t_{tb} according to Milnes and Perrochet [10] (on the
 267 abscissa) versus the ones resulting from TRS (on the ordinate) .

268



269

270 Fig. 6 – Scatterplot of the recycled flow rate ratio RR_{max} according to Milnes and Perrochet [10] (on
 271 the abscissa) versus the ones resulting from TRS (on the ordinate).

272

273 4. Derivation of an empirical relationship for thermal 274 recycling

275 Thermal recycling can occur in the well doublets where the parameter X exceeds the
 276 value of 1, as stated in Eq. 1. The following properties influence the significance of this

277 phenomenon and the time scales for its occurrence: the flow rate, the well distance, the
 278 hydraulic conductivity and the gradient, the flow direction and the aquifer thickness.
 279 A similarity in the time scales can also be found among different setups, because well
 280 doublets characterized by a long thermal breakthrough time (t_{tb}) reach the asymptotical
 281 maximum thermal alteration after a long time. This was originally observed by Clyde and
 282 Madabhushi [29] for the thermal feedback in a well doublet in the absence of groundwater
 283 flow. In this case, the variation of the extracted water temperature is a function of the ratio
 284 between the time t and the breakthrough time t_{tb} :

$$285 \quad \frac{T_E(t) - T_l}{T_0 - T_l} = 0.34 \cdot \exp\left(-0.0023 \frac{t}{t_{tb}}\right) + 0.34 \cdot \exp\left(-0.109 \frac{t}{t_{tb}}\right) + 1.37 \cdot \exp\left(-1.33 \frac{t}{t_{tb}}\right) \quad \text{for } t > t_{tb}$$

286 **Equation 13**

287 The temperature plots represented in Fig. 3 and in the supporting information
 288 demonstrate that the pattern of thermal recycling in the presence of groundwater flow
 289 resembles an asymptotical exponential more closely than a sum of exponentials. A more
 290 suitable structure of the formula was therefore chosen:

$$291 \quad T_E(t) - T_0 = \Delta T \cdot \frac{RR_{\max}}{1 - RR_{\max}} \cdot \left[1 - \exp\left(m \cdot \frac{t}{t_{tb}}\right) \right] \quad \text{for } t > t_{tb}$$

292 **Equation 14**

293 In order to estimate the coefficient $m < 0$ of Eq. 14, a total number of 62 simulations with
 294 TRS was run, covering a wide range of the X parameter (from 1.27 to 63.67). The ranges
 295 of values for each parameter adopted in this study are reported in Tab. 2, and further data
 296 on these simulations are available in the supporting information. Two criteria were adopted
 297 for the choice of typical settings to be simulated:

- 298 - a better fit should be found for small and medium values of X , since larger ones are
 299 typical of an unsustainable thermal exploitation of the aquifer. For this purpose, a
 300 larger number of simulations were run with a small X (i.e. less than 10);

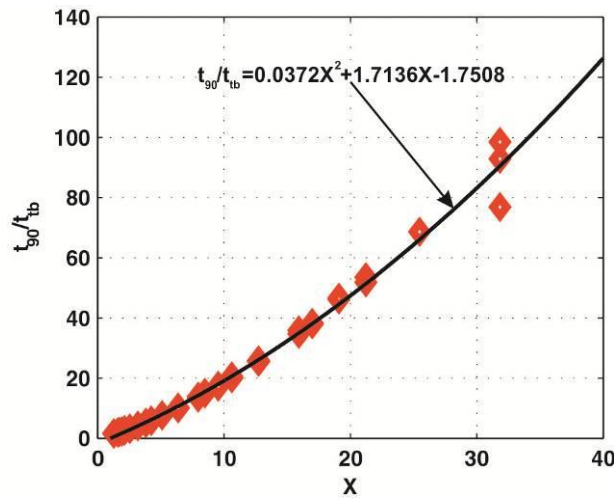
301 - for the same (or similar) value of X , different hydrogeological and well doublet
 302 parameters were adopted (e.g. a large well distance and a small hydraulic
 303 conductivity vs a small well distance and a large hydraulic conductivity), in order to
 304 verify if the coefficient m also depends on parameters other than X .

305 The fitting of the coefficient m of the asymptotic exponential function on Eq. 14 was
 306 performed by comparing the times at which 90% of the asymptotic maximum temperature
 307 change occurred (t_{90}). In particular, the ratio between t_{90} and the thermal breakthrough
 308 time t_{tb} can be approximated by a polynomial function of X (Fig. 7):

$$309 \quad \frac{t_{90}}{t_{tb}} = 0.0372X^2 + 1.7136X - 1.7508$$

310 **Equation 15**

311



312

313 **Fig. 7 – Plots of the ratio between t_{90} and the thermal breakthrough time t_{bt} against the non-**
 314 **dimensional parameter X .**

315

316 The interval function of the extracted water temperature was then calculated:

$$317 \quad \frac{T_E(t) - T_0}{\Delta T} = H(t - t_{tb}) \cdot \frac{RR_{\max}}{1 - RR_{\max}} \cdot \left[1 - \exp\left(\frac{\log(0.1)}{0.0372X^2 + 1.7136X - 1.7508} \cdot \frac{t}{t_{tb}} \right) \right]$$

318

Equation 16

319 where the parameters t_{tb} and RR_{\max} are calculated respectively with the formulae reported
320 in Eq.10 and 11, and $H(t - t_{tb})$ is the Heaviside function.

321 **5. Example of the applications of the models for thermal** 322 **recycling**

323 The mathematical methods provided in this paper (TRS and the formula reported in Eq.16)
324 can be used in the preliminary dimensioning of a GWHP. An example is shown in this
325 chapter, comparing the results of these methods with the output of numerical flow and heat
326 transport simulations with FEFLOW™. The results commented hereby are reported in Tab.
327 3. A small block of flats equipped with a GWHP needs a maximum cooling power of 210
328 kW during the cooling season (which lasts 120 days). A flow rate of 16.666 l/s with a
329 temperature difference of 3°C are therefore set. The aquifer is 30m thick, with a hydraulic
330 conductivity of 3×10^{-4} m/s and a hydraulic gradient of $5 \cdot 10^{-3}$. Given a thermal capacity of
331 the solid matrix $(\rho c)_s = 2.52 \frac{MJ}{m^3 K}$, a thermal capacity of water $(\rho c)_w = 4.2 \frac{MJ}{m^3 K}$ and an
332 effective porosity $n_e = 0.2$, the thermal retardation factor according to Eq.5 is $R_{th} = 3.4$. The
333 undisturbed aquifer temperature is 14°C and the upper limit temperature imposed by the
334 environmental authority is 20°C. A preliminary evaluation of the feasibility of the plant is
335 requested.

336 According to Eq.1, the minimum distance between wells to avoid thermal breakthrough
337 would be equal to 236 m, provided that they are aligned with the groundwater flow
338 direction. Since this is a very large value and it is not compatible with the extension of the
339 property, a value of $L = 100m$ is set. As reported in Tab. 3, this choice would result in a
340 thermal breakthrough time t_{tb} which is longer than the cooling season, and the extracted
341 water temperature will not experience any variation. Nevertheless, such a large distance

342 implies a noticeable increment of the cost of installation, and a reduction of this value
343 would be highly desirable. By setting $L = 40\text{ m}$, a shorter breakthrough time is obtained and
344 the asymptotical thermal alteration $T_i(\infty)$ in the injection well would be very close to the
345 limit imposed by the authority. However, a smaller variation occurs at the end of the
346 cooling season $T_i(t = 120d)$, that can also be calculated with the empirical relationship
347 reported in Eq. 16, and hence this configuration can also be considered as sustainable. A
348 slightly larger thermal alteration occurs if the groundwater flow is not aligned with the well
349 doublet (e.g. $\vartheta = 45^\circ$), which can be calculated both with FEFLOW™ and TRS with an
350 acceptable agreement between results, but not with Eq.16.

351 In general, an acceptable agreement is achieved between calculation results with different
352 methods, confirming the robustness of the models presented in this paper. As for the
353 thermal breakthrough time, a slight difference is observed between the value calculated by
354 FEFLOW™ and those obtained with TRS and the empirical formula.

355 Besides the results, the calculation times on a 30 years simulation on the same computer
356 (Pentium i7 4771 @3.50GHz with 12 GB DDR3 of RAM memory) are respectively of some
357 8 hours for FEFLOW™ and 10 seconds for TRS.

358 **6. Conclusions**

359 Ground Water Heat Pumps are a very convenient technology for the heating and cooling
360 of residential, commercial and industrial buildings, in particular for large plants, where the
361 cost of the well drilling and hydrogeological surveys have a minor incidence on the total
362 expense. In addition, noticeable CO₂ savings can be achieved, since the heat pump
363 operates at a very high COP. Usually groundwater is injected after the thermal exchange
364 to avoid the depletion of the aquifer, but this may cause a thermal feedback (if
365 groundwater is reinjected at a fixed temperature) or thermal recycling (if a fixed

366 temperature difference between production and injection well is set). Thermal feedback
367 has already been studied, through the development of numerical models and practical
368 formulae which estimate the time series of extracted water temperature (the injection
369 temperature is known *a priori*). A practical tool for the study of thermal recycling in the
370 presence of a regional groundwater flow has not yet been developed, which was the
371 objective of this work. A forward finite difference particle tracking procedure, based on
372 potential flow theory, was implemented in a MATLAB™ numerical code called TRS
373 (Thermal Recycling Simulator), in order to calculate the time series of the extracted and
374 injected water temperature in a GWHP with a constant flow rate and temperature
375 difference. Although the code manages to model a partial reinjection and an arbitrarily
376 oriented regional flow, the analysis focused on well doublets aligned with groundwater flow
377 with full reinjection of abstracted water, since this is a standard GWHP setting.

378 The modelling approach was validated through flow and heat transport simulations carried
379 out with FEFLOW™, the results of which were set as a benchmark. A good agreement
380 was observed for the most important outputs (water temperature time series, pathlines,
381 thermal breakthrough times), except for plants characterized by a very strong thermal
382 recycling, which would however be unsustainable in practice. A practical formula for
383 estimating the time evolution of groundwater temperature was then deduced, that would
384 further speed up the calculation times, while achieving a good agreement both with the
385 TRS code and with the finite-element numerical simulations.

386 The implemented mathematical models can be used for the design of small GWHPs with
387 conservative parameter values, for the feasibility assessment of larger plants, or for
388 mapping the suitability for GWHP installations on large areas, thus fostering the diffusion
389 of open loop shallow geothermal installations.

390

391

References

- 392 [1] J.W. Lund, D.H. Freeston, T.L. Boyd, Direct utilization of geothermal energy 2010
393 worldwide review, *Geothermics*, 40 (2011) 159-180.
- 394 [2] M. Antics, R. Bertani, B. Sanner, Summary of EGC 2013 Country Update Reports on
395 Geothermal Energy in Europe, in: *European Geothermal Conference, Pisa (Italy), 2013*,
396 pp. 1-18.
- 397 [3] P. Bayer, D. Saner, S. Bolay, L. Rybach, P. Blum, Greenhouse gas emission savings of
398 ground source heat pump systems in Europe: A review, *Renewable and Sustainable*
399 *Energy Reviews*, 16 (2012) 1256-1267.
- 400 [4] G. Florides, S. Kalogirou, Ground heat exchangers—A review of systems, models and
401 applications, *Renewable Energy*, 32 (2007) 2461-2478.
- 402 [5] A. Casasso, R. Sethi, Efficiency of closed loop geothermal heat pumps: A sensitivity
403 analysis, *Renewable Energy*, 62 (2014) 737-746.
- 404 [6] J.T. Chung, J.M. Choi, Design and performance study of the ground-coupled heat
405 pump system with an operating parameter, *Renewable Energy*, 42 (2012) 118-124.
- 406 [7] V. Wagner, P. Bayer, M. Kübert, P. Blum, Numerical sensitivity study of thermal
407 response tests, *Renewable Energy*, 41 (2012) 245-253.
- 408 [8] S. Lo Russo, G. Taddia, V. Verda, Development of the thermally affected zone (TAZ)
409 around a groundwater heat pump (GWHP) system: A sensitivity analysis, *Geothermics*, 43
410 (2012) 66-74.
- 411 [9] M.L. Brashears, Ground-water temperature on Long Island, New York, as affected by
412 recharge of warm water, *Economic Geology*, 36 (1941) 811-828.
- 413 [10] E. Milnes, P. Perrochet, Assessing the impact of thermal feedback and recycling in
414 open-loop groundwater heat pump (GWHP) systems: a complementary design tool,
415 *Hydrogeol J*, 21 (2013) 505-514.

- 416 [11] A.C. Gringarten, J.P. Sauty, A theoretical study of heat extraction from aquifers with
417 uniform regional flow, *J Geophys Res*, 80 (1975) 4956-4962.
- 418 [12] M.J. Lippmann, C.F. Tsang, Ground-Water Use for Cooling: Associated Aquifer
419 Temperature Changes, *Ground Water*, 18 (1980) 452-458.
- 420 [13] S. Al-Zyoud, W. Rühaak, I. Sass, Dynamic numerical modeling of the usage of
421 groundwater for cooling in north east Jordan – A geothermal case study, *Renewable*
422 *Energy*, 62 (2014) 63-72.
- 423 [14] H.J.G. Diersch, FEFLOW. Finite Element Modeling of Flow, Mass and Heat Transport
424 in Porous and Fractured Media, Springer-Verlag, Berlin Heidelberg, 2014.
- 425 [15] A. Galgaro, M. Cultrera, Thermal short circuit on groundwater heat pump, *Applied*
426 *Thermal Engineering*, 57 (2013) 107-115.
- 427 [16] S. Lo Russo, M.V. Civita, Open-loop groundwater heat pumps development for large
428 buildings: A case study, *Geothermics*, 38 (2009) 335-345.
- 429 [17] G.P. Beretta, G. Coppola, L.D. Pona, Solute and heat transport in groundwater
430 similarity: Model application of a high capacity open-loop heat pump, *Geothermics*, 51
431 (2014) 63-70.
- 432 [18] J. Hecht-Méndez, N. Molina-Giraldo, P. Blum, P. Bayer, Evaluating MT3DMS for heat
433 transport simulation of closed geothermal systems, *Ground Water*, 48 (2010) 741-756.
- 434 [19] R. Sethi, A. Di Molfetta, Heat transport modeling in an aquifer downgradient a
435 municipal solid waste landfill in Italy, *American Journal of Environmental Sciences*, 3
436 (2007) 106-110.
- 437 [20] J. Poppei, G. Mayer, R. Schwarz, Groundwater Energy Designer (GED) -
438 Computergestütztes Auslegungstool zur Wärme und Kältenutzung von Grundwasser
439 [Computer assisted design tool for the use of heat and cold from groundwater], in,
440 Bundesamt für Energie BFE, Switzerland, 2006, pp. 1-71.

- 441 [21] F. Stauffer, P. Bayer, P. Blum, N. Molina-Giraldo, W. Kinzelbach, Thermal use of
442 shallow groundwater, CRC Press - Taylor and Francis Group, 2013.
- 443 [22] O.D.L. Strack, Groundwater Mechanics, Prentice-Hall, Englewood Cliffs, NJ (USA),
444 1988.
- 445 [23] J. Luo, P.K. Kitanidis, Fluid residence times within a recirculation zone created by an
446 extraction–injection well pair, J Hydrol, 295 (2004) 149-162.
- 447 [24] G. Ferguson, Potential use of particle tracking in the analysis of low-temperature
448 geothermal developments, Geothermics, 35 (2006) 44-58.
- 449 [25] G. de Marsily, Quantitative hydrogeology, Academic Press, San Diego (CA, USA),
450 1986.
- 451 [26] A. Casasso, R. Sethi, Groundwater Engineering research group, Politecnico di Torino
452 - DIATI, <http://areweb.polito.it/ricerca/groundwater/software/TRS.html>, access date:
453 October 22nd, 2014
- 454 [27] DHI-WASY, FEFLOW IFM plugins,
455 [http://www.feflow.com/existing_ifm_modules.html?&no_cache=1&tx_ttnews\[tt_news\]=28&t](http://www.feflow.com/existing_ifm_modules.html?&no_cache=1&tx_ttnews[tt_news]=28&tx_ttnews[year]=2011)
456 [x_ttnews\[year\]=2011](http://www.feflow.com/existing_ifm_modules.html?&no_cache=1&tx_ttnews[tt_news]=28&tx_ttnews[year]=2011), access date: October 20th, 2014
- 457 [28] C.G. Clyde, G.V. Madabhushi, Spacing of wells for heat pumps, Journal of Water
458 Resources Planning & Management - ASCE, 109 (1983) 203-212.
- 459

Tables

Quantity	Symbol	Value	Unit
Domain length	-	5000	m
Domain width	-	3000	m
Thickness of the domain	-	120	m
Thickness of the aquifer	b	15÷100	m
(default value)		20	m
Effective porosity	n_e	0.02÷0.2	-
(default value)		0.2	-
Total porosity (equal to the effective porosity)	n	0.02÷0.2	-
(default value)		0.2	-
Isotropic hydraulic conductivity of the aquifer layers	K	$10^{-4} \div 10^{-3}$	m/s
(default value)		10^{-4}	m/s
Isotropic hydraulic conductivity of the other layers	K	10^{-8}	m/s
Longitudinal dispersivity	α_L	0.1	m
Transverse dispersivity	α_T	0.01	m
Well doublet discharge	Q_w	0.01	m ³ /s
Volumetric heat capacity of solid	$(\rho c)_s$	0.63÷12.6	MJ/(m ³ K)
(default value)		2.52	
Volumetric heat capacity of water	$(\rho c)_w$	4.2	MJ/(m ³ K)
Thermal conductivity of solid	λ_s	0.01	W/(mK)
Thermal conductivity of water	λ_w	0.01	W/(mK)
Boundary conditions (thermal) on all slices	T	14	°C
Initial conditions (thermal) on all slices	T_0	14	°C
Boundary conditions (hydraulic) on all slices (western side)	-	225	m
Boundary conditions (hydraulic) on all slices (eastern side)	-	175÷220	m
(default value)	-	200	m
Hydraulic gradient imposed	J	0.001÷0.005	-
(default value)		0.005	-
Problem class	-	Saturated	-
Aquifer type	-	Unconfined	-
Unconfined aquifer option	-	Free and movable	-
Error tolerance	-	$5 \cdot 10^{-4}$	-
Upwinding scheme	-	No upwind (Galerkin FEM)	-
Number of elements of the 3D mesh	-	288333	-
Number of nodes of the 3D mesh	-	151060	-
Number of slices of the 3D mesh	-	28	-
Number of layers of the 3D mesh	-	27	-

487

488 **Tab. 1 – Summary of the model settings adopted in the simulation with FEFLOW for the validation of**
489 **the TRS numerical code.**

490

491

Parameter	Symbol	Values
Hydraulic conductivity	k	10-5÷10-3 m s ⁻¹
Hydraulic gradient	J	0.001÷0.02
Aquifer thickness	b	5÷50 m
Well distance	L	10÷200 m
Flow rate	Q_w	0.001÷0.05 m ³ s ⁻¹

492

493 **Tab. 2 – Parameter values adopted for the simulations with the TRS code, in order to fit the**
 494 **parameters of Eq. 14.**

495

L [m]	ϑ [°]	X	Quantity	Analytical formulae	TRS	FEFLOW™
100	0°	2.36	t_{tb} [d]	228.274 ^a	228.278	243.000
			RR_{max}	0.234 ^b	0.232	n.a.
			$T_l(\infty)$ [°C]	17.916 ^c	17.906 ^c	17.759 ^e
			$T_l(t = 120d)$ [°C]	17.000 ^d	17.000	17.000
40	0°	5.89	t_{tb} [d]	27.510 ^a	27.504	26.000
			RR_{max}	0.491 ^b	0.484	n.a.
			$T_l(\infty)$ [°C]	19.892 ^c	19.814 ^c	19.943 ^e
			$T_l(t = 120d)$ [°C]	18.871 ^d	19.043	18.624
40	45°	-	t_{tb} [d]	n.a.	26.474	24.000
			RR_{max}	n.a.	0.512	n.a.
			$T_l(\infty)$ [°C]	n.a.	20.150 ^c	20.326 ^e
			$T_l(t = 120d)$ [°C]	n.a.	19.254	18.693

496

497 ^a calculated with Eq. 10

498 ^b calculated with Eq. 11

499 ^c calculated with Eq. 12

500 ^d calculated with Eq. 16

501 ^e calculated after 10950 days (30 years)

502 **Tab. 3 – Application of the TRS numerical code and of the practical formula for thermal recycling:**
 503 **results with different plant setups.**

504

505

Acronyms

Acronym	Meaning
COP	Coefficient of Performance
EER	Energy Efficiency Ratio
GED	Groundwater Energy Design
GWHP	Ground Water Heat Pump
PT	Particle Tracking
TRS	Thermal Recycling Simulator

506

507

Symbols (Greek letters)

Symbols	Meaning	Unit of measure
ΔT	Temperature difference between injected and extracted water	K, °C
ϑ	Groundwater flow angle (measured counter-clockwise with respect to the conjunction of the extraction and the injection well)	rad
ρ_s	Density of the solid matrix of the aquifer	kg m ⁻³
ρ_w	Density of groundwater	kg m ⁻³
Ω	Complex potential	m ³ s ⁻¹

508

509

Symbols (Latin letters)

Symbols	Meaning	Unit of measure
b	Saturated thickness of the aquifer	m
c_s	Specific heat of the solid matrix of the aquifer	$\text{J m}^{-3} \text{K}^{-1}$
c_w	Specific heat of groundwater	$\text{J m}^{-3} \text{K}^{-1}$
J	Hydraulic gradient of the aquifer	-
k	Hydraulic conductivity of the aquifer	ms^{-1}
L	Distance between the extraction and the injection well	m
m	Angular coefficient in the empirical correlation of extracted water temperature vs time	-
n	Number of injected particles that have already reached the extraction well at a certain time	-
N	Total number of injected particles	-
n_e	Effective porosity	-
n_{\max}	Maximum number of injected particles that reach the extraction well	-
X	Non-dimensional thermal breakthrough parameter	-
Q_w	Well flow rate	$\text{m}^3 \text{s}^{-1}$
Q_{gw}	Groundwater flow rate vector	$\text{m}^2 \text{s}^{-1}$
R_{th}	Thermal retardation factor	-
r_w	Well radius	m
RF	Reinjected flow rate fraction	-
$RR(t)$	Fraction of the injected flow rate that returns to the extraction well	-
RR_{\max}	Maximum fraction of the injected thermally altered water flow rate that returns to the extraction well	-
t	Time	s
t_{90}	Time for which 90% of the maximum thermal alteration in the extraction well is reached	s
t_p	Recycled particle travel time	s
t_{tb}	Thermal breakthrough time	s
T_0	Undisturbed groundwater temperature	K, °C
$T_E(t)$	Extracted water temperature	K, °C
$T_I(t)$	Injected water temperature	K, °C
v_e	Groundwater effective velocity	ms^{-1}
v_{e-th}	Effective velocity of the thermal alteration in groundwater	ms^{-1}
z	Planar position expressed as a complex number	m
z_E	Planar position of the extraction well	m
z_I	Planar position of the injection well	m